# **Charge-based Separation of Microparticles Using AC Insulator- Based Dielectrophoresis**

Seyed Mojtaba Tabarhoseini,<sup>1,#</sup> Akshay Shridhar Kale,<sup>2,#</sup> Peter Michael Koniers,<sup>1</sup> Anna Claire Boone,<sup>1</sup> Joseph Bentor,<sup>1</sup> Adam Boies,<sup>2</sup> Hui Zhao,<sup>3</sup> Xiangchun Xuan<sup>1,\*</sup>

<sup>&</sup>lt;sup>1</sup>Department of Mechanical Engineering, Clemson University, Clemson, SC 29634, USA

<sup>&</sup>lt;sup>2</sup>Department of Engineering, University of Cambridge, Cambridge CB2 1PZ, United Kingdom

<sup>&</sup>lt;sup>3</sup>Department of Mechanical Engineering, University of Nevada, Las Vegas, NV 89154, USA

<sup>&</sup>lt;sup>#</sup> S.M.T. and A.S.K. contributed equally to this paper.

<sup>\*</sup> Corresponding author. Email: xcxuan@clemson.edu (Dr. Xuan). Fax: 864-656-7299.

### **ABSTRACT**

Surface charge is an important property of particles. It has been utilized to separate particles in microfluidic devices, where dielectrophoresis (DEP) is often the driving force. However, current DEP-based particle separations based on charge difference work only for particles of similar sizes. They become less effective and may even fail for a mixture of particles differing in both the charge and size. We demonstrate that our recently developed AC insulator-based dielectrophoresis (AC iDEP) technique can direct microparticles toward charge-dependent equilibrium positions in a ratchet microchannel. Such charge-based particle separation is controlled by the imposed AC voltage frequency and amplitude, but nearly unaffected by the size of either type of particle in the mixture except for the time required to achieve an effective separation. This AC iDEP technique may potentially be used to focus and separate submicron or even nanoparticles because of its virtually "infinite" channel length.

### INTRODUCTION

The separation of target particles (either biological cells or non-biological beads) from a mixture is often a necessary step prior to analysis for chemical, environmental and biomedical applications. <sup>1-3</sup> It has been increasingly implemented in microfluidic devices since late 1990s because of the advantages over their benchtop counterparts. <sup>4-7</sup> The force(s) that drives the particle separation in these devices can be externally imposed and/or internally induced. <sup>8-11</sup> The former type of active methods relies on the electric, <sup>12,13</sup> acoustic, <sup>14,15</sup> or magnetic <sup>16,17</sup> field-driven phoretic motion to manipulate particles to different flow paths. The latter type of passive methods exploits the flow-induced migration to direct particles to different equilibrium positions. <sup>18-23</sup> Integrating multiple separation methods of either of these two types into one microfluidic device has been demonstrated to further improve the separation metrics. <sup>24-26</sup> Many of these single- or multi-mode microfluidic separations are label free and based on the difference in the intrinsic properties of particles such as size and shape. <sup>27-30</sup>

Surface charge is another intrinsic property of particles.<sup>31,32</sup> It affects the interaction among particles and hence the stability of particle suspension.<sup>33,34</sup> It also affects the force between particles and the charged walls of the container, and hence the adsorption onto these walls.<sup>35,36</sup> Surface charge has been utilized to separate particles, where electric field must be involved and the separation has been demonstrated in both a batch process and a continuous flow. The batchwise separation takes place along the axis of time including capillary electrophoresis<sup>37</sup> and electrical field flow fractionation,<sup>38</sup> where particles of dissimilar charges are eluted out of the column at different times. The Lapizco-Encinas group has recently developed another batchwise separation based on the difference in particle charge, which arises from the competition of dielectrophoresis (DEP) and charge-dependent electrophoresis of particles around insulating posts.<sup>39,40</sup> This group

later reported that the consideration of nonlinear electrophoresis enables an accurate modeling of particle migration and retention in insulator-based electrokinetic systems under both DC<sup>41</sup> and DC-biased AC electric fields.<sup>42</sup>

Several continuous-flow methods have also been presented for the separation of particles by charge along the axis of space. Free-flow electrophoresis is one such method, where a transverse electric field is imposed upon a pressure-driven flow to divide the particles into different lanes based on their electrophoretic velocities. 43 In another continuous method, a bidirectional pressure and electric field-driven flow can be tuned to selectively trap particles with a specific charge into the recirculating zone in a converging-diverging microchannel. <sup>44</sup> DEP has also been demonstrated for charge-based particle separation in a continuous flow. Our group utilized the wall-induced DEP-like lift force to separate particles and cells with similar sizes by charge in a DC electric fielddriven electroosmotic flow through a w-shaped microchannel. 45 We also achieved a continuousflow separation of particles by charge both inside the reservoir of a straight microchannel via reservoir-based DEP<sup>46</sup> and in a double-spiral microchannel via curvature induced DEP.<sup>47</sup> In a later paper, Lentz et al.<sup>48</sup> proposed the use of low-frequency cyclical electric potentials to switch between trapping and streaming DEP for a continuous charge-based particle separation. In another paper, Calero et al.<sup>49</sup> reported a charge-based separation of microparticles in a deterministic lateral displacement separation device with imposed DC and AC electric fields orthogonal to the fluid flow.

All existing DEP-based separations by particle charge work only for particles of equal or similar sizes. They become less effective and may even fail when the size of one type of particle in the mixture is unfavorably larger (or smaller) because of the strong dependence of DEP on the particle volume. <sup>50,51</sup> In our recent paper, we have developed an AC insulator-based dielectrophoresis (AC

iDEP) technique that sacrifices time to gain a virtually "infinite" channel length for particle and cell focusing along the centerline of a ratchet microchannel.<sup>52</sup> We demonstrate in this work that AC iDEP can direct particles toward charge-dependent equilibrium positions, either along the channel centerline or at the base of ratchets, regardless of their sizes. Such charge-based particle separation is dependent on the imposed AC voltage frequency and amplitude. We also propose a theory to explain the mechanism and develop a numerical model to simulate the process of this AC iDEP focusing and separation of particles.

### **MATERIALS AND METHODS**

# **Experimental Setup**

Figure 1a shows a picture of the microchannel, which was fabricated in polydimethylsiloxane (PDMS) using the standard soft-lithography technique.<sup>53</sup> The channel is 8 mm long between the two end-channel reservoirs with a uniform depth of 35 μm. It comprises along each sidewall an array of 20 triangular ratchets with a spatial period of 250 μm. The widest part of the channel is 500 μm, and the narrowest part at the throat formed by the opposing ratchet tips is 100 μm. Plain (Sigma-Aldrich) and fluorescent (Bangs Laboratories) 5 μm-diameter polystyrene particles, hereafter referred to as Sigma and Bangs particles, respectively, were each re-suspended into 0.25 mM phosphate buffer solution for the investigation of AC iDEP focusing. They were also mixed in 0.25 mM phosphate buffer for the demonstration of AC iDEP separation of particles by charge. In addition, 10 μm-diameter Sigma (plain) and Bangs (fluorescent) particles were mixed with 5 μm-diameter Bangs (fluorescent) and Sigma (plain) particles, respectively, to examine the role of particle size in charge-based AC iDEP separation. The particle concentration was kept at 10<sup>6</sup>–10<sup>7</sup> particles per ml. To prevent the adhesion of particles to the channel walls and the aggregation of

particles, Tween 20 (Fisher Scientific) was added to each prepared particle solution at a concentration of 0.5% (in volume) followed by an agitation in a vortex mixer (Fisher Scientific).

Prior to experiment, the liquid heights in the two end-channel reservoirs were balanced to minimize the influence of pressure-driven fluid flow on particle motion. A function generator (Agilent Technologies) along with a high-voltage amplifier (Trek) was used to supply square-wave AC voltages across the ratchet microchannel with varying frequencies and amplitudes. The imposed root-mean-square AC voltage was kept no more than 400 V (the corresponding electric field is 500 V/cm on average) in all tests, under which Joule heating and other nonlinear electrokinetic effects have been found insignificant in our previous studies. 54-56 The motion of particles was recorded in the middle of the channel using a CCD Camera (Nikon DSQi1Mc) connected to an inverted microscope (Nikon Eclipse TE2000U, Nikon Instruments). The obtained digital images were post-processed using the Nikon imaging software (NIS-Elements AR 2.30). The Image J software (National Institute of Health) was used to obtain the probability density function (PDF) of particles across the channel width. The electrokinetic mobility of particles was determined from the electrokinetic velocity, which was measured using the particle tracking velocimetry.<sup>57,58</sup> Briefly, we tracked 3-5 individual particles traveling along the centerline of a straight rectangular microchannel, where DEP vanishes, under 50, 100 and 200 V/cm. The electrokinetic velocity of each particle for each applied electric field was determined by dividing its traveling distance with the time duration. The electrokinetic mobility was then obtained from the slope of the average electrokinetic velocity for all particles vs. electric field.

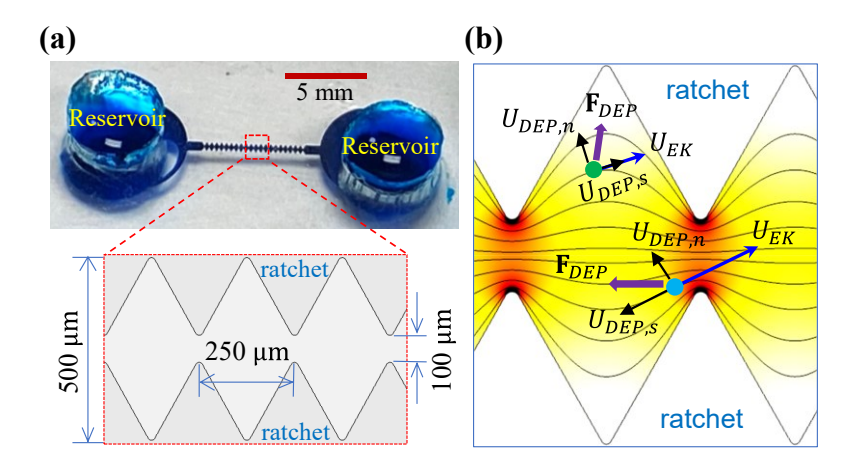


**Figure 1.** AC iDEP focusing and separation of particles in a ratchet microchannel: (a) Picture of a fabricated microchannel (filled with food dye for clarity) with the inset highlighting the dimensions of the ratchets; (b) Illustration of the particle focusing and separation mechanisms, where the nonuniform electric field (see the contour of electric field strength around the ratchets, the darker color the larger magnitude) induced dielectrophoretic force,  $\mathbf{F}_{DEP}$ , produces both a stream-wise particle motion,  $U_{DEP,S}$  and a cross-stream particle motion,  $U_{DEP,n}$ . The combination of  $U_{DEP,S}$  and the streamwise electrokinetic particle velocity,  $U_{EK}$ , determines how far a particle can travel within one half period of the AC voltage application.  $U_{DEP,n}$  directs a faster-moving particle (which can travel through the throat formed by the opposing ratchet tips) toward the channel center and a slower-moving particle (which remains within the wider region of the channel) toward the base of ratchets for simultaneous focusing and separation. The background lines show the electric field lines or equivalently the fluid streamlines.

# **Theoretical Analysis**

The schematic in Figure 1b illustrates the mechanisms for AC iDEP focusing and separation of particles in a ratchet microchannel. The nonuniform electric field induced by the insulating ratchets (see the contour of electric field strength in Figure 1b, the darker color the larger magnitude) produces a dielectrophoretic force,  $\mathbf{F}_{DEP}$ , which for a spherical particle is given by,<sup>59</sup>

$$\mathbf{F}_{DEP} = \frac{1}{4}\pi d^3 \varepsilon \text{Re}\{f_{CM}\} \nabla \mathbf{E}^2$$
 (1)

where d is the particle diameter,  $\varepsilon$  is the fluid permittivity, Re $\{f_{CM}\}$  denotes the real part of the complex Clausius-Mossotti factor, and  $\mathbf{E}$  is the root-mean-square electric field. For low-frequency AC electric fields (<100 kHz),<sup>60</sup> Re $\{f_{CM}\}$  =  $(\sigma_p - \sigma_f)/(\sigma_p + 2\sigma_f)$  with  $\sigma_p$  and  $\sigma_f$  being the electric conductivity values of the particle and fluid, respectively. Therefore, the dielectrophoretic

force directs the particle with  $\sigma_p - \sigma_f < 0$  towards the lower electric field region (i.e., negative DEP) and the one with  $\sigma_p - \sigma_f > 0$  towards the higher electric field region (i.e., positive DEP). Polystyrene microparticles used in this work experience negative DEP regardless of their size or charge, whose velocity,  $\mathbf{U}_{DEP}$ , can be broken down in the streamline coordinates,  $^{16,61}$ 

$$\mathbf{U}_{DEP} = \mu_{DEP} \nabla \mathbf{E}^2 = U_{DEP,s} \hat{\mathbf{s}} + U_{DEP,n} \hat{\mathbf{n}} = \mu_{DEP} \left( \frac{\partial \mathbf{E}^2}{\partial s} \hat{\mathbf{s}} + 2 \frac{\mathbf{E}^2}{\Re} \hat{\mathbf{n}} \right)$$
(2)

$$\mu_{DEP} = \frac{d^2 \varepsilon}{12\eta} \operatorname{Re} \{ f_{CM} \} \tag{3}$$

In the above,  $\mu_{DEP}$  is the dielectrophoretic mobility,  $U_{DEP,s}$  is the streamwise component of dielectrophoretic velocity with  $\hat{\mathbf{s}}$  being the unit vector in the streamline direction,  $U_{DEP,n}$  is the cross-stream component with  $\hat{\mathbf{n}}$  being the unit vector in the normal-line direction,  $\Re$  is the radius of curvature of the streamline (equivalent to the electric field line<sup>62</sup>), and  $\eta$  is the fluid viscosity.

As viewed from the particle velocity analysis in Figure 1b,  $U_{DEP,n}$  competes with the streamwise particle velocity, which is a summation of  $U_{DEP,s}$  and the electrokinetic velocity,  $U_{EK}$ , leading to a cross-stream focusing effect on particles. The equilibrium position, however, depends on if a particle can travel through the throat between the opposing ratchet tips, where the electric field reaches the local minimum at the channel center due to symmetry, in each (time) period of the AC voltage. Specifically, the particle that completes (at least) one half spatial period of the ratchets within one half (time) period of the AC voltage can pass through the throat and is hence directed toward the center of the channel (see the velocity analysis for the particle near the throat in Figure 1b). This AC iDEP centerline focusing of particles has been demonstrated in our previous paper.<sup>52</sup> In contrast, the particle that travels less than one half spatial period of the ratchets within one half period of the AC voltage remains in the wider region of the channel at any time and is eventually directed toward the base of the closest ratchet (see the velocity analysis for the particle

near the ratchet base in Figure 1b), where the local electric field attains the lowest value (see the electric field contour in Figure 1b). Such AC iDEP baseline focusing was not recognized in our previous study.<sup>52</sup>

The critical condition that divides the above AC iDEP centerline and baseline particle focusing can thus be approximately estimated from,

$$\frac{U_{EK}}{f} = \frac{\mu_{EK}E}{f} = T \tag{4}$$

if the contribution of  $U_{DEP,S}$  is assumed small compared to that of  $U_{EK}$  in the streamwise particle velocity. In the above,  $U_{EK} = \mu_{EK}E$  with  $\mu_{EK} > 0$  being the electrokinetic mobility, f is the frequency of the AC voltage, and T is the spatial period of the ratchets. Specifically,  $U_{EK}/f > T$ leads to centerline focusing while  $U_{EK}/f < T$  leads to baseline focusing. As T is fixed in a ratchet channel, eq 4 indicates that  $\mu_{EK} = \varepsilon (\zeta_p - \zeta_w)/\eta$ , where  $\zeta_p$  and  $\zeta_w$  are the particle and wall zeta potentials,  $^{31}$  E and f can be tuned either individually or mutually to alter the AC iDEP focusing position. Moreover, as  $\mu_{EK}$  is independent of the size of a particle unless the particle has a close fit to the channel<sup>63,64</sup> or experiences nonlinear electrophoresis,<sup>65,66</sup> particle size is not expected to be a factor affecting the equilibrium position of AC iDEP focusing. Therefore, by tuning E and f of the AC electric field, a particle with a larger value of  $\mu_{EK}$  can achieve a centerline focusing while one with a smaller value of  $\mu_{EK}$  instead experiences a baseline focusing, yielding a chargebased AC iDEP separation in the ratchet microchannel. The particle parameters, i.e.,  $\mu_{EK}$  and particle size, and as well the AC electric field parameters, i.e., E and f, will all be experimentally studied to understand their effects on AC iDEP focusing and separation of particles. These effects will also be numerically investigated to further validate the theory developed above.

### **Numerical Simulation**

A 2D numerical model was developed in the COMSOL Multiphysics<sup>®</sup> software to simulate the AC iDEP focusing and separation of particles in a ratchet microchannel. It solves only the Laplace equation in the fluid domain to obtain the electric field distribution, which is then used in the "Particle Tracing" module to compute the particle velocity,  $^{52}$   $\mathbf{U}_P$ , via,

$$\mathbf{U}_{P} = \mathbf{U}_{EK} + \lambda \mathbf{U}_{DEP} = \mu_{EK} \mathbf{E} + \lambda \mu_{DEP} \nabla \mathbf{E}^{2}$$
 (5)

Here,  $\lambda$  is the correction factor introduced by our group<sup>61</sup> for the particle size effect on DEP because the formula for the dielectrophoretic force in eq 1 and in turn that for the dielectrophoretic mobility,  $\mu_{DEP}$ , in eq 3 are only valid for particles whose size is much smaller than the characteristic length of electric field variations. This condition breaks down near the ratchet tips and becomes more problematic for larger particles. We set the correction factor in the model to 0.7 and 0.6 for 5- and 10 µm-diameter particles, respectively, regardless of the particle charge. The electrokinetic mobility,  $\mu_{EK}$ , was experimentally measured as  $2.5 \times 10^{-8}$  m<sup>2</sup>/(V·s) and  $1.0 \times 10^{-8}$ m<sup>2</sup>/(V·s) for the Sigma and Bangs particles, respectively, each of which was found insensitive to the size of the particles under test. These two values were found consistent with the reported electrokinetic mobilities for similar particles in similar buffer solutions in the literature. 46,47,67 The dielectrophoretic mobility,  $\mu_{DEP}$ , was calculated from eq 3, where the fluid viscosity,  $\eta$ , and permittivity,  $\varepsilon$ , were each assumed equal to the value for water at room temperature. The fluid electric conductivity,  $\sigma_f$ , was experimentally measured as 55  $\mu$ S/cm. The particle electric conductivity,  $\sigma_p$ , was calculated from  $\sigma_p = 4\sigma_s/d$  with  $\sigma_s = 1$  nS being the suggested surface conductance for polystyrene microparticles.<sup>68</sup> It is important to note that this method fails to calculate the electric conductivity of submicron and nanoparticles, which depends on both the surface charge and size of the particles.<sup>69</sup> Our model considered 150 particles that were initially distributed within the middle four ratchets of the channel using a built-in random number generator.

### RESULTS AND DISCUSSION

# **AC Voltage Frequency-Tuned Particle Focusing Position**

Figure 2a shows the snapshot images of 5 μm Sigma particles taken at different time instants in the middle of the ratchet microchannel under 200 V AC voltage (i.e., 250 V/cm AC electric field on average) of 0.5 Hz frequency. Particles are randomly dispersed within the channel at the initial time step when the AC voltage is off. They start traveling back and forth through the ratchets while being pushed away from the ratchet tips by negative DEP once the AC voltage is turned on. This AC iDEP centerline focusing effect grows over time, which is properly simulated by the 2D numerical model (see Figure 2a). The experimentally and numerically obtained PDF plots for particles in Figure 2b also demonstrate the increasing AC iDEP centerline focusing over the time of AC voltage application. In contrast, when the AC voltage frequency is increased to 2 Hz while its amplitude remains unvaried, particles are no longer able to pass through any throat between the opposing ratchet tips within one period of the AC voltage and hence migrate toward the base of the ratchets because of the action of negative DEP. This AC iDEP baseline focusing of particles also increases over time as evidenced by the experimental and numerical images in Figure 2c as well as the experimental and numerical PDF plots in Figure 2d.

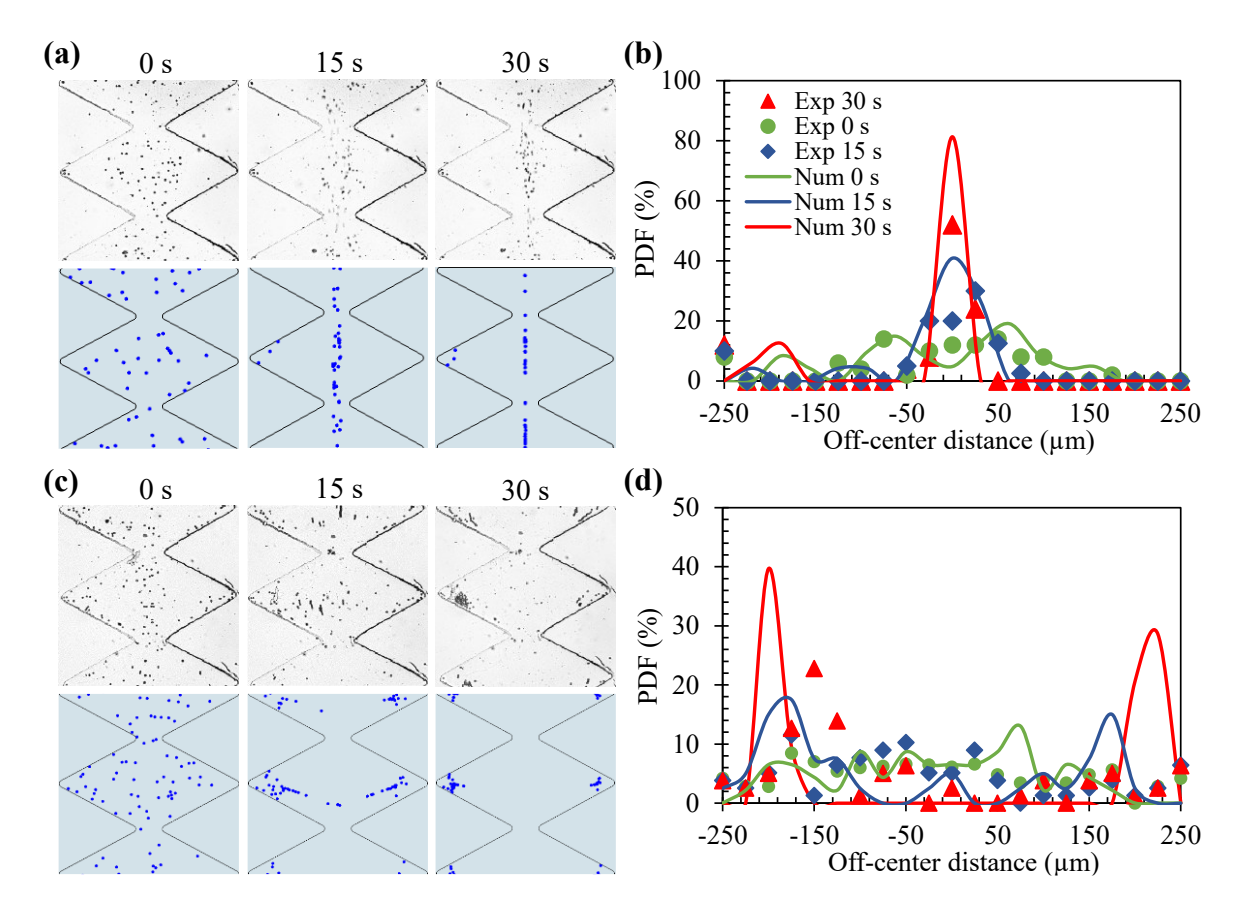


**Figure 2.** Frequency-tuned AC iDEP focusing of 5 μm-diameter Sigma particles under 200 V AC voltage: comparison of the experimental (upper row) and numerical (lower row) images obtained at different time instants for 0.5 Hz (a) and 2.0 Hz (c) AC voltages; comparison of the experimental (symbols) and numerical (lines) particle PDF plots obtained at different time instants for 0.5 Hz (b) and 2.0 Hz (d) AC voltages.

We note that such AC voltage frequency-tuned particle focusing positions in Figure 2 are consistent with the critical condition in eq 4. Specifically, considering the electrokinetic velocity of Sigma particles under 250 V/cm,  $U_{EK} = \mu_{EK}E = 0.63$  mm/s, we get  $U_{EK}/f = 1.3$  mm and 0.31 mm for 0.5 and 2 Hz AC voltages, respectively. The former distance satisfies  $U_{EK}/f > T$ , where T = 0.25 mm is the spatial period of the ratchets in our microchannel (see Figure 1a), leading to AC iDEP centerline focusing of particles (Figures 2a and 2b). Our recent study<sup>52</sup> indicates that the value of  $U_{EK}/f$  should be about four times larger than that of T in order that even those Sigma particles that travel adjacent to either channel sidewall (at a slower  $U_{EK}$  with a

longer traveling distance) can pass through the throat of the channel within one half period of the AC voltage application. That observation is again consistent with the values obtained here. The particle traveling distance  $U_{EK}/f = 0.31$  mm for 2 Hz AC voltage is roughly equal to the ratchet period, which, however, can become smaller than that if the contribution of negative  $U_{DEP,s}$  to the streamwise particle velocity is considered in eq 4. The result of this consideration is the AC iDEP baseline focusing of particles (Figures 2c and 2d).

# **Electrokinetic Velocity-Dependent Particle Focusing Position**

Figure 3 compares the experimental images of 5 μm Sigma and 5 μm Bangs particles, respectively, which were all taken 60 s after the application of AC voltage with varying frequencies and amplitudes. Two trends are observed for each type of particle in Figure 3: one is that with the increasing frequency of AC voltage of any amplitude, the particle focusing position shifts from the channel centerline, if available, to the base of the ratchets and/or the baseline focusing gets improved. This trend for Bangs particles can be explained using the same mechanism as that for Sigma particle in the preceding section, i.e., the decreased particle travel distance within one half period of a higher-frequency AC voltage. The other trend is that with the increase of AC voltage amplitude from 100 to 300 V, the particle focusing position shifts from the ratchet base to channel centerline for Sigma particles at the higher frequencies (see 1.0 Hz) and Bangs particles at the lower frequencies (see 0.1 Hz). This trend is caused by the increased particle travel distance within one half period of a higher-amplitude AC voltage. For the other cases, the AC iDEP centerline and baseline focusing effects become more pronounced for Sigma and Bangs particles, respectively, with the increase of AC voltage amplitude because of the resulting stronger DEP.

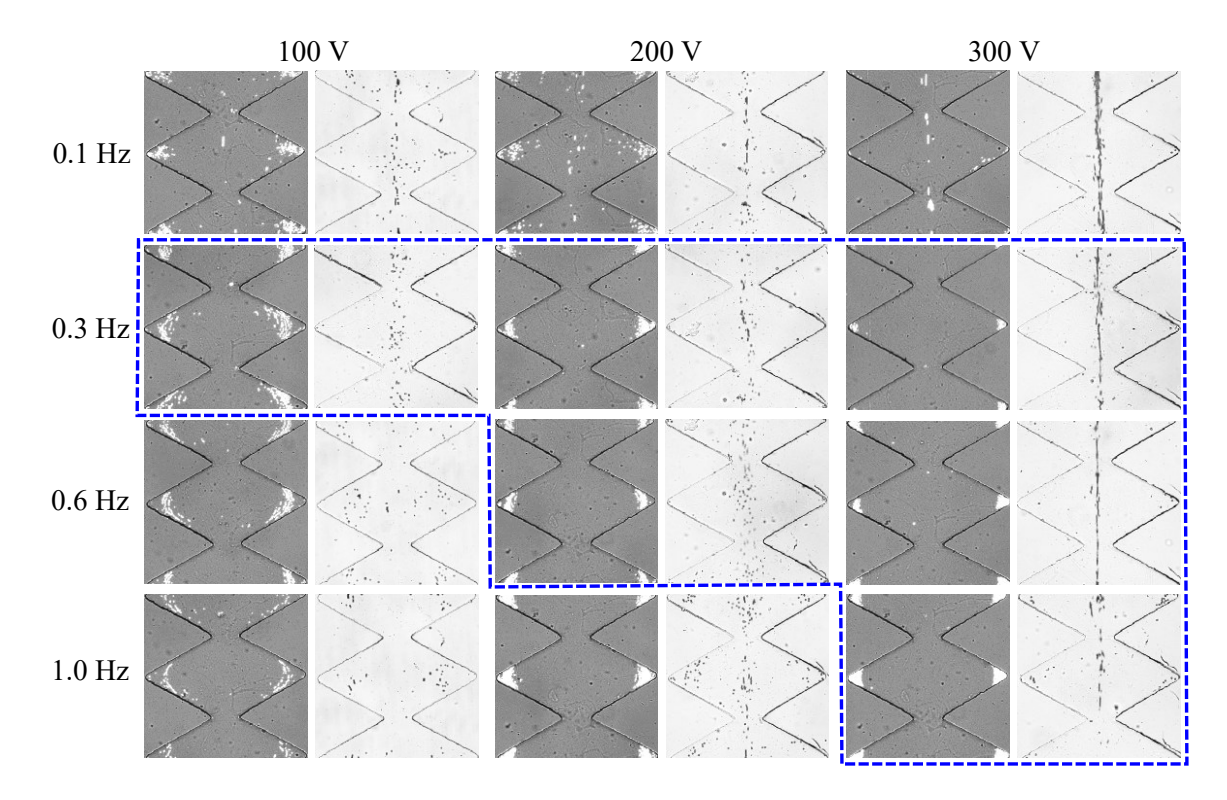


**Figure 3.** Experimental images of 5 μm-diameter Bangs (bright) and Sigma (dark) particles, respectively, in the ratchet microchannel 60 s after the application of AC voltages of varying frequencies and amplitudes. The dashed line box highlights the frequency and amplitude window, where Bangs and Sigma particles experience AC iDEP baseline and centerline focusing, respectively, and hence a charge-based separation is available.

Another phenomenon that can be clearly seen from Figure 3 is the dissimilar AC iDEP focusing patterns for Sigma and Bangs particles. Our measured electrokinetic mobility values indicate that Sigma particles move faster than Bangs particles under the same AC voltage and carry less negative surface charges. As the surface charge and AC voltage amplitude together determine the electrokinetic particle velocity, the particle images in Figure 3 can be viewed to demonstrate the electrokinetic velocity-dependent AC iDEP focusing position. Moreover, there exist several combinations of AC voltage frequency and amplitude in Figure 3 (highlighted by the dashed-line box), under which Bangs and Sigma particles experience AC iDEP baseline and centerline focusing, respectively. In other words, these two types of particles can be physically separated

from each other based on the difference in surface charge if they are mixed in the ratchet microchannel subject to AC iDEP.

# **Demonstration of Charge-based Particle Separation**

Figure 4 shows the experimental and numerical images for the AC iDEP separation of the mixture of 5 µm Sigma and 5 µm Bangs particles over time. The imposed AC voltage is 300 V with a 0.6 Hz frequency. Both types of particles are randomly scattered throughout the ratchet microchannel at 0 s. After the AC voltage is turned on, the action of negative DEP directs the faster-moving Sigma particles toward the channel centerline and the slower-moving Bangs particles toward the ratchet base, respectively. These distinct migrations are each consistent with the observation of individual particles under the same AC voltage in Figure 3. They take place, as explained above, because Sigma particles can pass through the channel throat(s) within each period of the AC voltage application while Bangs particles do not. Such centerline and baseline focusing effects both grow over time, leading to an increased separation gap between the two types of particles. The time development of this charge-based particle separation is reasonably simulated by the numerical model (Figure 4, lower row). We counted the number of each type of particles from the sequential images in the ImageJ software and used the data to calculate the efficiency (defined as the number of target particles inside a specific zone over the total number of target particles) and purity (defined as the number of target particles inside a specific zone over the total number of particles inside the same zone). It is found that our separation can achieve over 90% efficiency and purity for both Sigma (in the zone around the channel centerline) and Bangs (in the zone near the ratchet base) particles.

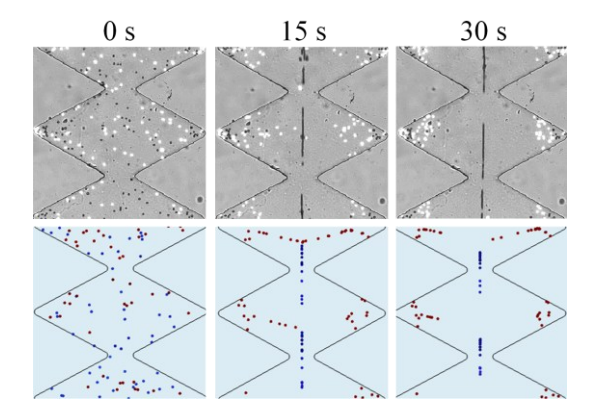


**Figure 4.** Experimental (upper row) and numerical (lower row) images illustrating the time development of charge-based AC iDEP separation of 5  $\mu$ m Sigma (dark) and Bangs (bright) particles under 300 V AC voltage of 0.6 Hz frequency.

# Effects of the AC Voltage Frequency and Amplitude

Figure 5 compares the experimental images for the charge-based separation of 5 µm Sigma and 5 µm Bangs particles over a range of AC voltage frequencies and amplitudes. Under a fixed AC voltage frequency of 0.6 Hz, Sigma particles form a compact stream along the channel centerline at 200 V and maintain this focusing state when the AC voltage amplitude is increased to 400 V. Meanwhile, Bangs particles still partially spread from the ratchet base to the channel centerline at 200 V but experience an apparently improved baseline focusing with the increase of AC voltage amplitude because of the strengthened dielectrophoretic force (see eq 1). Similarly, under a fixed AC voltage amplitude of 300 V, Sigma particles exhibit a strong AC iDEP centerline focusing at 0.2 Hz and can remain focused even when the AC voltage frequency is increased to 1 Hz. In contrast, Bangs particles undergo an enhanced AC iDEP baseline focusing with the increase of AC voltage frequency, which is consistent with the observation in Figure 3 because they are further confined to the wider region of the channel in a shortened period of a higher-frequency AC voltage. Therefore, our AC iDEP charge-based particle separation can be optimized by tuning the AC voltage frequency and/or amplitude.

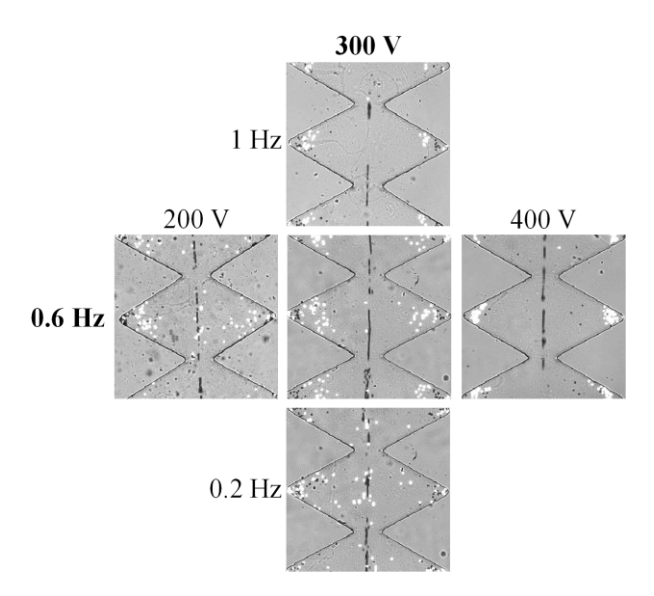


**Figure 5.** Experimental images (taken 60 s after the AC voltage application) illustrating the effects of AC voltage frequency (labeled to the left of images at each row) and amplitude (labeled on top of the images at each column) on the charge-based AC iDEP separation of 5 μm-diameter Sigma (dark) and Bangs (bright) particles in the ratchet microchannel.

### **Role of the Particle Size**

Figure 6 compares the experimental images over time for the mixture of 10 μm Sigma/5 μm Bangs particles, 5 μm Sigma/5 μm Bangs particles, and 5 μm Sigma/10 μm Bangs particles, respectively, in the ratchet microchannel under 300 V AC voltage of 1 Hz frequency. The charge-based AC iDEP separation of Sigma and Bangs particles is achieved in all cases regardless of their sizes. However, replacing 5 μm particles of either type in the mixture with 10 μm ones of the same type is seen from Figure 6 to significantly shorten the time required for particle separation. This accelerated AC iDEP separation is attributed to the greater dielectrophoretic mobility of a larger particle (see eq 3). Moreover, it is interesting to observe that increasing the size of the fastermoving Sigma particle leads to an even quicker separation than increasing the size of the slowermoving Bangs particles. Specifically, a complete AC iDEP separation of 10 μm Sigma and 5 μm Bangs particles takes only 5 s while that of 5 μm Sigma and 10 μm Bangs particles needs 20 s as compared to 40 s for the mixture of 5 μm Sigma and 5 μm Bangs particles. These numbers together

imply that the centerline focusing of Sigma particles is more difficult to implement than the baseline focusing of Bangs particles, and hence has a greater influence on the time development of AC iDEP separation. We attribute such a phenomenon to the higher requirement for centerline focusing, where every single particle, especially those that move slowly near the base of the ratchet, must pass through the throat of the channel within one period of AC voltage. In contrast, the AC iDEP baseline focusing requires that only those particles moving fast around the channel centerline be unable to travel through the throat.

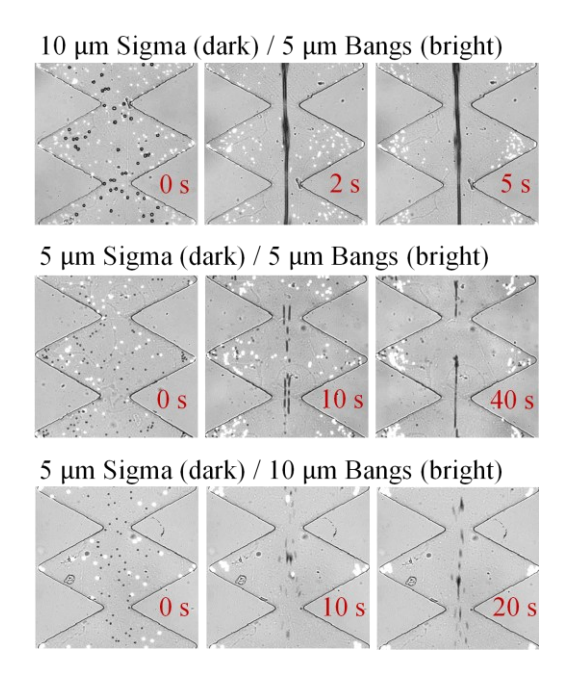


**Figure 6.** Experimental images illustrating the effect of particle size (labeled on top of each row of images) on the time (labeled on each image) development of AC iDEP separation of Sigma (dark) and Bangs (bright) particles under 300 V AC voltage of 1 Hz frequency.

# **CONCLUSIONS**

We have demonstrated that our recently developed AC iDEP technique<sup>52</sup> can direct a particle toward either the centerline or baseline of a ratchet microchannel. This switching of particle focusing position depends on if the particle can pass through the throat between the ratchet tips within one period of the AC voltage application. It is thus a function of the electrokinetic particle

velocity and AC voltage frequency as reflected by a proposed simple formula in eq. 4. We have utilized this electrokinetic velocity-dependent AC iDEP focusing technique to separate a mixture of equal-sized particles based on the difference in their charges. Such a separation can be optimized by tuning the AC voltage amplitude and/or frequency. It is, however, unaffected by the particle size except that increasing the size of either type of particle in the mixture significantly accelerates the separation process because of the enhanced dielectrophoretic motion. We have also developed a 2D numerical model, which is found to simulate the experimentally observed AC iDEP focusing and separation of particles with a reasonable agreement. It is admitted that our experimental matrix is relatively small with only two sizes of particles carrying two different surface charges. However, our experimental demonstration along with the theoretical analysis and numerical simulation together should be sufficient to justify the principle for the proposed AC iDEP particle focusing and separation technique. This technique is envisioned to find applications in the manipulation and analysis of submicron or even nanosized particles considering its practically "infinite" channel length, which will be our future work. We will also investigate in future work if this technique works for the separation of biological cells.

### **AUTHOR CONTRIBUTIONS**

S.M.T., P.M.K., A.C.B., and J.B. performed the experiment; S.M.T. and A.S.K. performed the simulation and analysis; S.M.T. and A.S.K. wrote the manuscript; A.B., H.Z. and X.X. supervised the project and edited the manuscript.

### **ACKNOWLEDGEMENTS**

This work was supported in part by NSF under grant numbers CBET-2100772 and CBET-2127825 (X.X.) as well as CBET-2127852 and DMR-2314340 (H.Z.). It was also supported in part by Clemson University through the Creative Inquiry Program (X.X.) and the Engineering and Physical Sciences Research Council (EPSRC) Impact Acceleration Award (IAA) (A.S.K.).

# **REFERENCES**

- [1] Aubry, G.; Lee, H. J.; Lu, H. Advances in microfluidics: Technical innovations and applications in diagnostics and therapeutics. *Anal. Chem.* **2023**, *95*, 1, 444–467
- [2] Diaz-Armas, G. G.; Cervantes-Gonzalez, A. P.; Martinez-Duarte, R.; Perez-Gonzalez, V. H. Electrically driven microfluidic platforms for exosome manipulation and characterization. *Electrophoresis* 2022, 43, 327–339.
- [3] Battat, S.; Weitz, D. A.; Whitesides, G. M. An outlook on microfluidics: the promise and the challenge. *Lab Chip* **2022**, *22*, 530-536.
- [4] Karimi, A.; Yazdi, S.; Ardekani, A. M. Hydrodynamic mechanisms of cell and particle trapping in microfluidics. *Biomicrofluid.* **2013**, *7*, 021501.
- [5] Sajeesh, P.; Sen, A. K. Particle separation and sorting in microfluidic devices: a review. *Microfluid. Nanofluid.* **2014**, *17*, 1–52.
- [6] Shields IV, C. W.; Reyes, C. D.; López, G. P. Microfluidic cell sorting: a review of the advances in the separation of cells from debulking to rare cell isolation. *Lab Chip* 2015, 15, 1230-1249.

- [7] Antfolk, M.; Laurell, T. Continuous flow microfluidic separation and processing of rare cells and bioparticles found in blood A review. *Anal. Chim Acta* **2017**, *965*, 9-35.
- [8] Kulrattanarak, T.; van der Sman, R. G. M.; Schroën, C. G. P. H.; Boom, R. M. Classification and evaluation of microfluidic devices for continuous suspension fractionation. Adv. Colloid Interface Sci. 2008, 142, 53–66.
- [9] Liang, W.; Liu, J.; Yang, X.; Zhang, Q.; Yang, W.; Zhang, H.; Liu, L. Microfluidic-based cancer cell separation using active and passive mechanisms. *Microfluid. Nanofluid.* **2020**, 24, 26.
- [10] Zhang, S.; Wang, Y.; Onck, P.; den Toonder, J. A concise review of microfluidic particle manipulation methods. *Microfluid. Nanofluid.* **2020**, *24*, 24.
- [11] Al-Ali, A.; Waheed, W.; Abu-Nada, E.; Alazzam, A. A review of active and passive hybrid systems based on dielectrophoresis for the manipulation of microparticles. *J. Chromatography A* **2022**, *1676*, 463268.
- [12] Wu, M.; Ozcelik, A.; Rufo, J.; Wang, Z.; Fang, R.; Huang, T. J. Acoustofluidic separation of cells and particles. *Microsyst. Nanoeng.* **2019**, *5*, 32.
- [13] Novotny, J.; Lenshof, A.; Laurell, T. Acoustofluidic platforms for particle manipulation. *Electrophoresis* **2022**, *43*, 804-818.
- [14] Xuan, X. Recent advances in continuous-flow particle manipulations using magnetic fluids. *Micromachines* **2019**, *10*, 744.
- [15] Pesch, G. R.; Du, F. A review of dielectrophoretic separation and classification of non-biological particles. *Electrophoresis* **2021**, *42*, 134-152.
- [16] Xuan, X. Recent advances in direct current electrokinetic manipulation of particles for microfluidic applications. *Electrophoresis* 2019, 40, 2484-2513.

- [17] Chong, W. H.; Leong, S. S.; Lim, J. K. Design and operation of magnetophoretic systems at microscale: Device and particle approaches. *Electrophoresis* **2021**, *42*, 2303-2328.
- [18] Zhang, J.; Yan, S.; Yuan, D.; Alici, G.; Nguyen, N. T.; Warkiani, M. E.; ro Fundamentals and applications of inertial microfluidics: a review. *Lab Chip* **2016**, *16*, 10–34.
- [19] Stoecklein, D.; Di Carlo, D. Nonlinear microfluidics. Anal. Chem. 2019, 91, 296–314.
- [20] Xiang, N.; Ni, Z. Inertial microfluidics: current status, challenges, and future opportunities. *Lab Chip* **2022**, *22*, 4792-4804.
- [21] Lu, X.; Liu, C.; Hu, G.; Xuan, X. Particle manipulations in non-Newtonian microfluidics: a review. *J. Colloid Interface Sci.* **2017**, *500*, 182-201.
- [22] Tian, F.; Feng, Q.; Chen, Q.; Liu, C.; Li, T.; Sun, J. Manipulation of biomicro/nanoparticles in non-Newtonian microflows. *Microfluid. Nanofluid.* **2019**, *23*, 68.
- [23] Zhou, J.; Papautsky, I. Viscoelastic microfluidics: progress and challenges. *Microsyst.*Nanoeng. **2020**, *6*, 113.
- [24] Yan, S.; Zhang, J.; Yuan, D.; Li, W. Hybrid microfluidics combined with active and passive approaches for continuous cell separation. *Electrophoresis* **2017**, *38*, 238-249.
- [25] Cha, H.; Fallahi, H.; Dai, Y.; Yuan, D.; An, H.; Nguyen, N. T.; Zhang, J. Multiphysics microfluidics for cell manipulation and separation: a review. *Lab Chip* **2022**, *22*, 423-444.
- [26] Song, Y.; Li, D.; Xuan, X. Recent advances in multi-mode microfluidic separation of particles and cells. *Electrophoresis* **2023**, *44*, 910-937.
- [27] Gossett, D. R.; Weaver, W. M.; Mach, A. J.; Hur, S C.; Tse, H. T.; Lee, W.; Amini, H.; Di Carlo, D. Label-free cell separation and sorting in microfluidic systems. *Anal. Bioanal. Chem.* **2010**, *397*, 3249–3267.

- [28] Tang, W.; Jiang, D.; Li, Z.; Zhu, L.; Shi, J.; Yang, J.; Xiang, N. Recent advances in microfluidic cell sorting techniques based on both physical and biochemical principles. *Electrophoresis* **2019**, *40*, 930-954.
- [29] Nasiri, R.; Shamloo, A.; Ahadian, S.; Amirifar, L.; Akbari, J.; Goudie, M. J.; Lee, K.; Ashammakhi, N.; Dokmeci, M. R.; Di Carlo, D.; Khademhosseini, A. Microfluidic-based approaches in targeted cell/particle separation based on physical properties: Fundamentals and applications. *Small* **2020**, *16*, 2000171.
- [30] Wu, Y.; Chattaraj, R.; Ren, Y.; Jiang, H.; Lee, D. Label-free multitarget separation of particles and cells under flow using acoustic, electrophoretic, and hydrodynamic forces. *Anal. Chem.* **2021**, *93*, 7635–7646.
- [31] Hunter, R. J. Zeta Potential in Colloid Science, Academic Press, New York 1981.
- [32] Jiang, T.; Chen, X.; Ren, Y.; Tang, D.; Jiang, H. Dielectric characterization and multistage separation of various cells via dielectrophoresis in a bipolar electrode arrayed device. *Anal. Chem.* **2021**, *93*, 10220-10228.
- [33] Lyklemma, J. Fundamentals of Interface and Colloid Science, Academic Press, Cambridge, UK 1991.
- [34] Russel, W. B.; Saville, D. A.; Schowalter, W. R. *Colloidal Dispersions*, Cambridge University Press, Cambridge, UK **1992**.
- [35] Probstein, R. F. *Physicochemical Hydrodynamics*. John Willey and Sons, Hoboken **1994**.
- [36] Kirby, B. *Micro- and Nanoscale Fluid Mechanics: Transport in Microfluidic Devices*, Cambridge University Press, New York, USA **2010**.

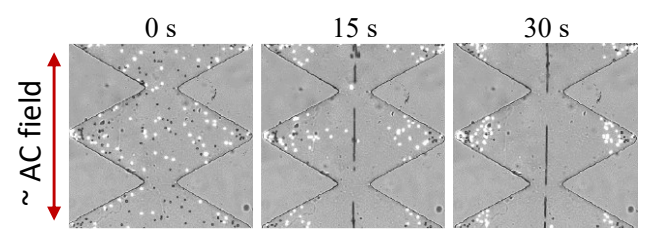
- [37] Rodriguez, M. A.; Armstrong, D. W. Separation and analysis of colloidal/nano-particles including microorganisms by capillary electrophoresis: a fundamental review. *J. Chromatogr. B* **2004**, *800*, 7–25.
- [38] Giddings, J. C. Field-flow fractionation: analysis of macromolecular, colloidal, and particulate materials. *Science* **1993**, *206*, 1456–1465.
- [39] Polniak, D. V.; Goodrich, R.; Hill, N.; Lapizco-Encinas, B. H. Separating large microscale particles by exploiting charge differences with dielectrophoresis. *J. Chromatography A* **2018**, *1545*, 84–92.
- [40] Hill, N.; Lapizco-Encinas, B. H. Continuous flow separation of particles with insulator-based dielectrophoresis chromatography. *Anal. Bioanal. Chem.* **2020**, *412*, 3891–3902.
- [41] Vaghef-Koodehi, A.; Dillis, C.; Lapizco-Encinas, B. H. High-resolution charge-based electrokinetic separation of almost identical microparticles. *Anal. Chem.* **2022**, *94*, 6451-6456.
- [42] Ahamed, N. N. N.; Mendiola-Escobedo, C. A.; Ernst, O. D.; Perez-Gonzalez, V. H.; Lapizco-Encinas, B. H. Fine-tuning the characteristic of the applied potential to improve AC-iEK separations of microparticles. *Anal. Chem.* **2023**, *95*, 9914–9923.
- [43] Kohlheyer, D.; Eijkel, J. C. T.; van den Berg, A.; Schasfoort, R. B. M. Miniaturizing free-flow electrophoresis a critical review. *Electrophoresis* **2008**, *29*, 977–993.
- [44] Jellema, L. C.; Mey, T., Koster, S.; Verpoorte, E. Charge-based particle separation in microfluidic devices using combined hydrodynamic and electrokinetic effects. *Lab Chip* **2009**, *9*, 1914–1925.

- [45] Thomas, C.; Lu, X.; Todd, A.; Raval, Y.; Tzeng, T.; Song, Y.; Wang, J.; Li, D.; Xuan, X. Charge-based electrokinetic separation of particles and cells with similar sizes via the wall-induced electrical lift. *Electrophoresis* **2017**, *38*, 320-326.
- [46] Patel, S.; Qian, S.; Xuan, X. Reservoir-based dielectrophoresis (rDEP) for microfluidic particle separation by charge. *Electrophoresis* **2013**, *34*, 961-968.
- [47] Zhu, J.; Xuan, X. Curvature-induced dielectrophoresis for continuous separation of particles by charge in spiral microchannels. *Biomicrofluid.* **2011**, *5*, 024111.
- [48] Lentz, C. J.; Hidalgo-Caballero, S.; Lapizco-Encinas, B. H. Low frequency cyclical potentials for fine tuning insulator-based dielectrophoretic separations. *Biomicrofluid*. **2019**, *13*, No. 044114.
- [49] Calero, V.; Garcia-Sanchez, P.; Ramos, A.; Morgan, H. Combining DC and AC electric fields with deterministic lateral displacement for micro- and nano-particle separation. *Biomicrofluid.* 2019, 13, 054110.
- [50] Ramirez-Murillo, C. J.; de Los Santos-Ramirez, J. M.; Perez-Gonzalez, V. H. Toward low-voltage dielectrophoresis-based microfluidic systems: A review. *Electrophoresis* **2021**, *42*, 565-587.
- [51] Pohl, H. A. *Dielectrophoresis*, Cambridge University Press, Cambridge, **1978**.
- [52] Malekanfard, A.; Beladi-Behbahani, S.; Tzeng, T. R.; Zhao, H.; Xuan, X. AC insulator-based dielectrophoretic focusing of particles and cells in an "infinite" microchannel. *Anal. Chem.* **2021**, *93*, 5947-5953.
- [53] Malekanfard, A.; Ko, C. H.; Li, D.; Bulloch, L; Baldwin, A.; Wang, Y. N.; Fu, L. M.; Xuan, X. Experimental Study of Particle Electrophoresis in Shear-Thinning Fluids. *Phys. Fluids* 2019, 31, 022002.

- [54] Kale, A.; Song, L.; Lu, X.; Yu, L.; Hu, G.; Xuan, X. Electrothermal enrichment of submicron particles in an insulator-based dielectrophoretic microdevice. *Electrophoresis* 2018, 39, 887-896.
- [55] Malekanfard, A.; Liu, Z.; Zhao, H.; Song, Y.; Xuan, X. Interplay of induced charge electroosmosis and electrothermal flow in insulator-based dielectrophoresis. *Phys. Review Fluids* **2021**, *6*, 093702.
- [56] Xuan, X. Review of nonlinear electrokinetic flows in insulator-based dielectrophoresis: From induced charge to Joule heating effects. *Electrophoresis* **2022**, *43*, 167–189.
- [57] Bentor, J.; Dort, H.; Chitrao, R.; Zhang, Y.; Xuan, X. Nonlinear electrophoresis of dielectric particles in Newtonian fluids. *Electrophoresis* **2023**, *44*, 938-946.
- [58] Lomeli-Martin, A.; Ernst, O. D.; Cardenas-Benitez, B.; Cobos, R.; Khair, A. S.; Lapizco-Encinas, B. H. Characterization of the nonlinear electrophoretic behavior of colloidal particles in a microfluidic channel. *Anal. Chem.* **2023**, *95*, 6740–6747.
- [59] Lapizco-Encinas, B. H. On the recent developments of insulator-based dielectrophoresis: A review. *Electrophoresis* **2019**, *40*, 358-375.
- [60] Voldman, J. Electrical forces for microscale cell manipulation. *Annu. Rev. Biomed. Eng.*2006, 8, 425-454.
- [61] Zhu, J.; Xuan, X. Dielectrophoretic focusing of particles in a microchannel constriction using DC-biased AC electric fields. *Electrophoresis* **2009**, *30*, 2668-2675.
- [62] Cummings, E. B.; Griffiths, S. K.; Nilson, R. H.; Paul, P. H. Conditions for similitude between the fluid velocity and electric field in electroosmotic flow. *Anal. Chem.* **2000**, *72*, 11, 2526–2532.

- [63] Anderson, J. L. Colloid transport by interfacial forces, *Annu. Rev. Fluid. Mech.* **1989**, *21*, 61–99.
- [64] Xuan, X.; Raghibizadeh S.; Li, D.; Wall effects on electrophoretic motion of spherical polystyrene particles in a rectangular poly(dimethylsiloxane) microchannel. *J. Colloid Interface Sci.* **2006**, *296*, 743-748.
- [65] Ernst, O. D.; Vaghef-Koodehi, A.; Dillis, C.; Lomeli-Martin, A.; Lapizco-Encinas, B. H. Dependence of nonlinear electrophoresis on particle size and charge. *Anal. Chem.* 2023, 95, 6595–6602.
- [66] Cobos, R.; Khair, A. S. Nonlinear electrophoretic velocity of a spherical colloidal particle.
  J. Fluid Mech. 2023, 968, A14.
- [67] Liu, Z.; Li, D.; Saffarian, M.; Tzeng, T.; Song, Y.; Pan, X.; Xuan, X. Revisit of wall-induced lateral migration in particle electrophoresis through a straight rectangular microchannel: effects of particle zeta potential. *Electrophoresis* **2019**, *40*, 955-960.
- [68] Ermolina, I.; Morgan, H. The Electrokinetic Properties of Latex Particles: Comparison of Electrophoresis and Dielectrophoresis. *J. Colloid Interface Sci.* **2005**, *285*, 419–428.
- [69] Delgado, A. V.; González-Caballero, F.; Hunter, R. J.; Koopal, L. K.; Lyklema, J. J. Colloid Interface Sci. 2007, 309, 194–224.

# FOR TABLE OF CONTENTS ONLY



AC-iDEP separation of faster (dark) and slower (bright) moving microparticles regardless of size